

# Alkali ion scattering from Ag(001) and Ag thin films at low and hyperthermal energies

M.P. Ray, R.E. Lake, C.E. Sosolik\*

Department of Physics and Astronomy, Clemson University, 118 Kinard Laboratory, Clemson, South Carolina 29634, USA

## ARTICLE INFO

### Article history:

Received 19 September 2008  
Received in revised form 7 November 2008  
Available online 7 December 2008

### PACS:

85.30.De  
79.20.Rf  
34.50.-s  
34.35.+a

### Keywords:

Hot carriers  
Ion beam effects  
Ion-surface impact  
Ion scattering  
Semiconductor device measurement  
Hyperthermal energy

## ABSTRACT

We have investigated the scattering of  $K^+$  and  $Cs^+$  ions from a single crystal Ag(001) surface and from a Ag-Si(100) Schottky diode structure. For the  $K^+$  ions, incident energies of 25 eV to 1 keV were used to obtain energy-resolved spectra of scattered ions at  $\theta_i = \theta_f = 45^\circ$ . These results are compared to the classical trajectory simulation SAFARI and show features indicative of light atom-surface scattering where sequential binary collisions can describe the observed energy loss spectra. Energy-resolved spectra obtained for  $Cs^+$  ions at incident energies of 75 eV and 200 eV also show features consistent with binary collisions. However, for this heavy atom-surface scattering system, the dominant trajectory type involves at least two surface atoms, as large angular deflections are not classically allowed for any single scattering event. In addition, a significant deviation from the classical double-collision prediction is observed for incident energies around 100 eV, and molecular dynamics studies are proposed to investigate the role of collective lattice effects. Data are also presented for the scattering of  $K^+$  ions from a Schottky diode structure, which is a prototype device for the development of active targets to probe energy loss at a surface.

© 2009 Published by Elsevier B.V.

## 1. Introduction

Studies that utilize hyperthermal and low energy (1 eV–1 keV) ions to probe the fundamental dynamics of energy transfer at surfaces are unique as they bridge the gap between adsorption-dominated thermal energy (<1 eV) beam effects and the collision-dominated phenomena observed in the low-to-medium energy regimes (>1 keV). In particular, the small deBroglie wavelengths of the incident projectiles as well as the relatively large velocities perpendicular to the surface ensure that scattering trajectories are inherently classical and involve only a few atoms at the surface [1,2]. The knowledge gained from this type of work can be applied to the many technological processes that rely on ion-surface scattering, such as ion beam etching, desorption, and secondary ion mass spectrometry (SIMS).

Recent measurements of ion- and atom-surface interactions have revealed new phenomena that further highlight the need for continued fundamental studies. For example, the recent discovery of hot electron or chemicurrent-based pathways for energy loss at thin metal film surfaces [3–6] has initiated work into the role that electronic “potential energy” plays in the energy loss of

multiply charged ions [7,8]. In addition, new scattering studies have shown that projectiles with keV energies can exhibit unexpected diffraction effects [9–11].

Several seminal studies and references therein on alkali scattering at noble metal surfaces form the basis for our work [1,2,12,13]. Previous measurements on Ag surfaces have examined the (110) and (111) faces [14–17] and have focused primarily on normal incidence events and scattered angular distributions. We examine the energy-loss for alkali ions ( $K^+$  and  $Cs^+$ ) scattered from both a single crystal Ag(001) surface and from a thin film Ag Schottky diode structure. For this study, we have focused on specular scattered distributions obtained with the ions incident at  $45^\circ$  to the surface normal.

The organization of this paper is as follows. In Section 2 we describe our experimental apparatus and the preparation and fabrication steps for our single crystal sample and Schottky diode devices. The results of our scattering measurements are presented and discussed in Section 3. A summary of these data as well as prospects for future measurements are included in Section 4.

## 2. Experiment

Mass-resolved, monoenergetic ion beams are produced by a UHV low and hyperthermal energy ( $\sim 1$  eV–10 keV) ion beamline.

\* Corresponding author.

E-mail address: [sosolik@clemson.edu](mailto:sosolik@clemson.edu) (C.E. Sosolik).

Attached to the beamline is a UHV scattering chamber with a base pressure of  $8 \times 10^{-11}$  Torr. Located within the scattering chamber is a  $180^\circ$  electrostatic analyzer (ESA) attached to a channel electron multiplier for detecting scattered ions and a neutral particle detector (NPD) for detecting scattered neutral particles. The intensity of energy spectra obtained with the ESA and presented in this paper are energy-corrected to compensate for the ESA transmission function. Further details on our instrument can be found in a previous publication [18].

Prior to exposing the Ag(001) crystal to the ion beam, a cleaning cycle was performed consisting of a sputter with 500 eV  $\text{Ar}^+$  ions followed by an anneal to  $425^\circ\text{C}$  for 5 min. Following the cleaning cycle, the room temperature Ag(001) sample was exposed to beams of  $\text{K}^+$  and  $\text{Cs}^+$  ions ranging in incident energy from 10 eV to 2 keV. The beam was made incident on the sample at an angle of  $45^\circ$  relative to the surface normal along the  $\langle 110 \rangle$  azimuth. Energy-resolved spectra of the scattered beam were measured with the ESA over a range final angles. The ESA has an angular acceptance of  $3^\circ$ . Following sample exposure to the ion beam, Auger electron spectroscopy was performed to verify surface cleanliness.

Large area ultrathin film Ag/n-type Si(100) diode structures were used to study energy deposited into the target and gain insight into the creation of electron-hole pairs. These Schottky diode devices were fabricated in a custom-built deposition chamber that allows the substrate to be cooled to 120 K before deposition of the metal film. Previous studies have shown that Ag grows layer-by-layer with domains of (111) orientation at temperatures obtainable using liquid nitrogen [19–21]. The metal films were deposited using a thermal evaporation source resulting in flat, continuous, ultrathin metal films. Energy-resolved scattering measurements from one of these structures was obtained using the ESA for  $\text{K}^+$  ions incident at 1 keV.

### 3. Results and discussion

#### 3.1. K–Ag(001)

Using a  $\text{K}^+$  ion beam with incident energies ranging between 25 eV and 400 eV, energy- and angle-resolved spectra were obtained with the beam incident at an angle of  $45^\circ$  along the  $\langle 110 \rangle$  crystal azimuth. A representative spectrum is shown in Fig. 1 for

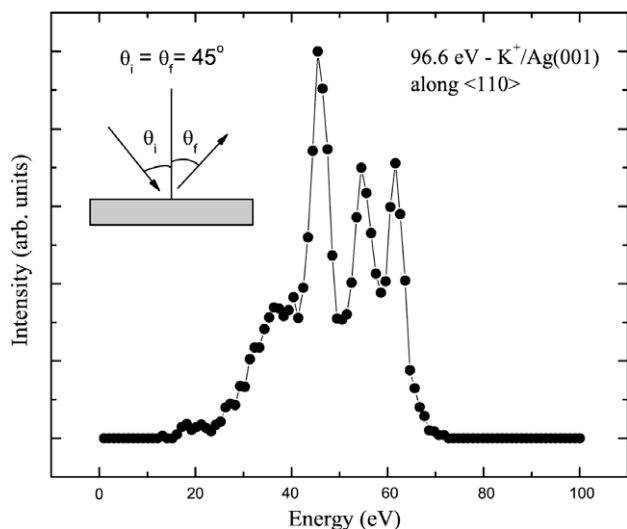


Fig. 1. An energy spectrum of  $\text{K}^+$  ions scattered from Ag(001) along the  $\langle 110 \rangle$  azimuth at 96.6 eV. The line connecting individual data points has been included as a guide to the eye. The scattering geometry is shown in the upper left.

a  $\sim 100$  eV  $\text{K}^+$  beam. In this spectrum as well as in those obtained at other energies, up to four distinct peaks in scattered intensity are observable. Previous results obtained on Ag and Cu surfaces indicate that these peaks should correspond to unique scattering trajectories at the Ag surface.

In order to explore the role of the simplest in-plane trajectory types in the K–Ag(001) system, a series of scattered spectra were obtained for a  $\sim 400$  eV incident beam at detector angles,  $\theta_f$ , between  $10^\circ$  and  $75^\circ$ . For these data, each energy-resolved spectrum was fit using a sum of Gaussian terms. The fits were used to construct the energy- $\theta_f$  plot shown in Fig. 2, where the reduced energy, i.e.  $E/E_{\text{inc}}$ , of the fitted peaks is plotted as a function of  $\theta_f$ . The lines shown in the figure correspond to quasi-single (QS) and quasi-double (QD) scattered energies as predicted using the binary collision approximation. The agreement between the predictions and the lowest and highest energy peaks at each  $\theta_f$  value present in the data is very good.

Beyond these two simple in-plane trajectory types, we would expect that additional out-of-plane trajectories contribute to these data. Given the small ( $\sim 2\%$ ) difference in the projectile-to-target mass ratio in this system ( $\mu \simeq 0.36$ ) and the Na–Cu system, it is reasonable to assume that the additional peaks seen are the double- and triple-zig-zag trajectories (DZZ and TZZ) previously identified for Na–Cu [2,22]. The classical trajectory simulation SAFARI was used to test this hypothesis [23]. Specifically, an interaction potential for an individual  $\text{K}^+$  ion and a Ag target atom was calculated using the STO-3G basis set in the GAUSSIAN 98 quantum chemistry package. This interaction potential was then used within the SAFARI simulation to obtain an accurate reproduction of the data. Trajectory analysis within these simulated data verify that a DZZ trajectory type does contribute to these data. For example, in the spectrum of Fig. 1, the DZZ trajectory type gives rise to the second highest scattered energy peak observed. A triple zig-zag trajectory type also appears in our simulations. However its contribution is limited to the low energy shoulder present on the QS peak, and its out-of-plane components penetrate into the  $\langle 110 \rangle$  channel of the surface as opposed to the top-layer only scattering seen in the Na–Cu TZZ trajectory. The SAFARI analysis also shows that the low energy shoulder on the QS peak contains a new zig-zag trajectory type that involves four surface atoms, i.e. a quadruple-zig-zag (QZZ). This particular trajectory did not appear in the Na–Cu sys-

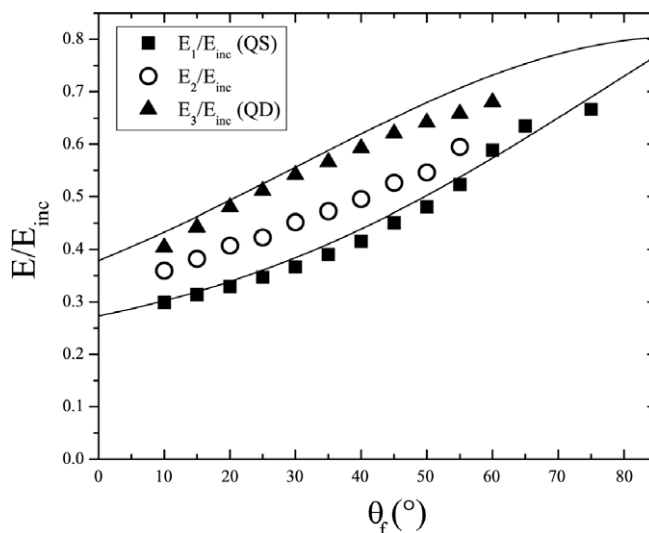


Fig. 2. A measured energy- $\theta_f$  plot for 400.9 eV incident  $\text{K}^+$  ions scattered Ag(001) along the  $\langle 110 \rangle$  azimuth at an incident angle of  $45^\circ$ . The lower and upper solid lines correspond to binary collision approximation predictions for QS and QD collisions, respectively.

tem, and SAFARI results indicate that it is due primarily to our choice of the  $\langle 110 \rangle$  azimuth for these measurements. That is, by scattering along this more close-packed, channeled direction at the Ag(001) surface, multiple out-of-plane trajectories become more probable [24].

### 3.2. Cs–Ag(001)

Energy loss in the scattering of Cs<sup>+</sup> from Ag(001) was investigated to probe the limits of our classical trajectory assumptions for a system where the projectile-to-target mass ratio is greater than one ( $\mu > 1$ ), i.e. a heavy atom-surface system. Historically, trajectory and binary collision-based results in the low and hyper-thermal energy regimes have focused almost entirely on light atom-surface systems. Here we have used Cs<sup>+</sup> ions at an incident angle of 45° on a Ag(001) surface along the  $\langle 110 \rangle$  azimuth with incident energies between 75 eV and 200 eV.

A representative scattered spectrum obtained for Cs<sup>+</sup> at ~100 eV is shown in Fig. 3. Integrating multiple spectra at this incident energy across a full range of final scattered angles, we obtain the spectrum shown in Fig. 4, which indicates that the scattering for this system is most intense at an angle greater than 45°. This supraspecular focusing is expected based on previous data in other heavy atom-surface systems [25], and it reflects the onset of a collective surface response for slow moving projectiles. To investigate the energy loss in more detail, energy- $\theta_f$  plots were constructed for the three incident energies shown in Fig. 5. The line shown in this figure corresponds to a QD trajectory as calculated within the binary collision approximation. The agreement between the data and the QD prediction indicates that the scattering is limited by its heavy atom nature, i.e. there is a limit on the total scattering angle,  $\theta_{TSA}^*$  possible for any single collision which is given by

$$\theta_{TSA}^* = \sin^{-1} \left( \frac{1}{\mu} \right). \quad (1)$$

For the case of Cs<sup>+</sup> scattering from Ag, this limit is  $\theta_{TSA}^* = 54^\circ$ . Therefore, a Cs<sup>+</sup> ion must undergo multiple collisions with Ag surface atoms in order to be detected within the supraspecular angular range indicated in Fig. 4. The simplest multiple collision trajectory type is the QD, and as Fig. 5 shows, it agrees well with the experimental results. However, our results obtained for incident energies

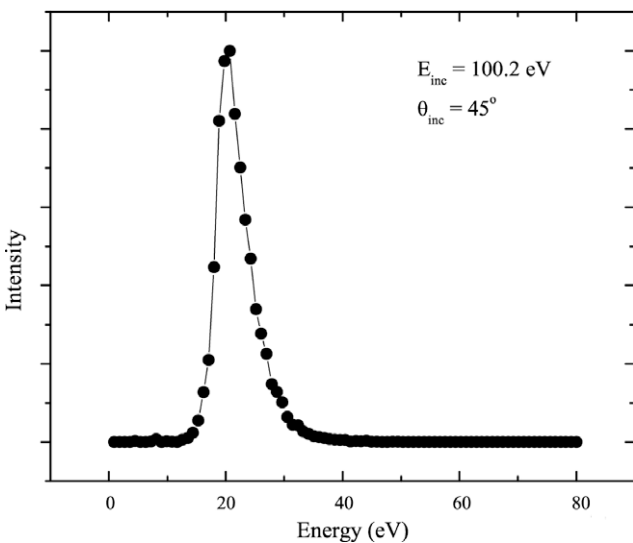


Fig. 3. A specular energy spectrum of Cs<sup>+</sup> ions scattered from Ag(001) along the  $\langle 110 \rangle$  azimuth at 100.2 eV with an incident angle of 45°. The line connecting individual data points has been included as a guide to the eye.

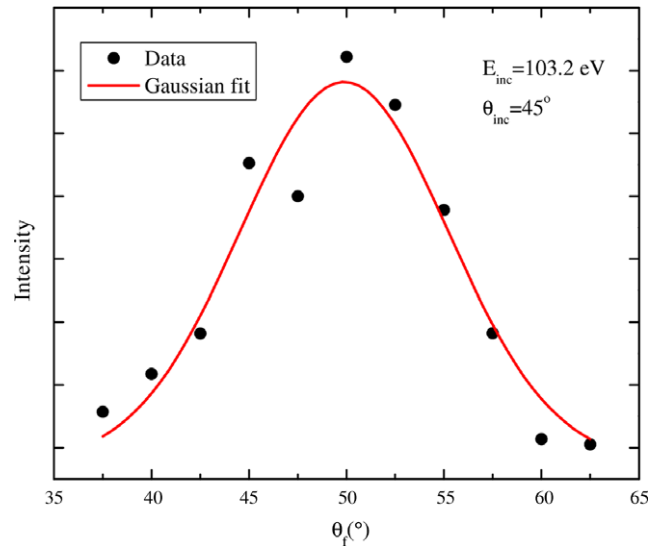


Fig. 4. An angular intensity spectrum obtained for Cs<sup>+</sup> ions scattered from Ag(001) along the  $\langle 110 \rangle$  azimuth at an incident angle of 45°. This spectrum was produced by integrating individual ESA spectra across a range of final scattered angles.

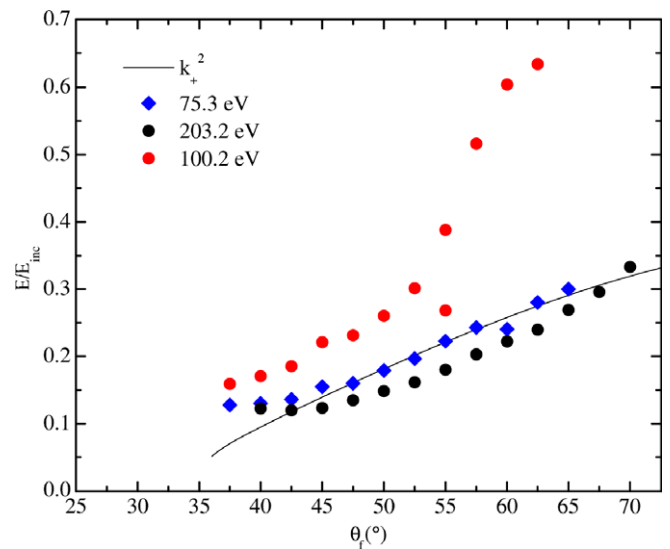


Fig. 5. A measured energy- $\theta_f$  plot for three incident energies of Cs<sup>+</sup> ion scattered from Ag(001) along the  $\langle 110 \rangle$  azimuth. All beams were incident at an angle of 45°. The line corresponds to the binary collision approximation prediction for a double collision.

near 100 eV show anomalous high energy peaks for scattered angles greater than 50°. Such an increase in the final scattered energy is not easily accounted for in the binary collision approximation. Previous data obtained by Yang et al. for Cs<sup>+</sup> scattered from a Si target also indicated a higher than expected scattered energy [26]. These authors attributed this increase to a collective lattice response that could be modeled with a large effective mass for the target atoms due to their bonding. The one caveat in comparing this result to our own data for Cs<sup>+</sup> is that we have only observed this response for incident energies near 100 eV.

We have attempted to interpret our results by simulating the Cs<sup>+</sup>–Ag(001) scattering events within SAFARI. The repulsive interaction or scattering potential required for the simulation was calculated within GAUSSIAN 98 using a Xe–Ag dimer. This noble gas–Ag atom dimer was chosen due to the inherent atomic number limitations of the STO-3G basis set used. However, the closed shell

electronic structure of Xe is essentially identical to singly ionized Cs and should return a very similar repulsive potential. The total energy for a Xe–Ag dimer was calculated as a function of the interatomic dimer separation. Calculations of isolated Xe and Ag atomic energies were then subtracted from the dimer values to obtain a separation-dependent repulsive Xe–Ag potential. This potential was used within SAFARI, but we were unable to reproduce the high scattered energies observed in the experimental data.

Within SAFARI the surface and near-surface region are generically modeled as a collection of atoms in a FCC lattice tied together with simple harmonic springs [27]. To test our hypothesis regarding a collective lattice response, the spring constants were increased systematically and all the calculated scattered energy peaks were seen to shift to higher energy. Nevertheless, the spring stiffening was unable to reproduce the trend seen in the data. This clearly does not discount the possibility that a collective response could rise to our observed results. The lattice treatment employed within SAFARI is over-simplified in the presence of a slow-moving projectile such as Cs, and a molecular dynamics or MD approach which more accurately treats the nature of bonding within the lattice is called for before a clear interpretation or reproduction of our results can be found.

### 3.3. K–Ag/n-Si(100)

There have been significant efforts over the past decade to probe the production of hot electron currents in ultrathin film devices, many of which incorporate Ag as their surface layer [28–31]. As many of the effects observed in these devices are related directly to the kinetic or energy loss effects of the ion-surface interaction, our tools for scattering spectroscopy are uniquely positioned to probe these systems. Therefore, we have fabricated prototype Schottky diode structures [32], and as a first measurement, have obtained energy-resolved scattered spectra for  $K^+$  ions.

Our Schottky diode devices are large area ultrathin film Ag layers deposited on n-type Si(100). In fabricating these metal semiconductor structures, our Sb-doped n-Si(100) substrates were prepared with a two hour anneal at 900 K, followed by a cooling to 120 K prior to Ag deposition. Current-voltage measurements on our as-fabricated devices have confirmed the presence of an

internal Schottky barrier. Atomic force microscopy measurements show that we can accurately deposit a metal film with a thickness in the range of 5–20 nm ( $\pm 1$  nm).

In Fig. 6 we show an energy-resolved scattered spectrum for 1 keV  $K^+$  ions scattered from a 20 nm Ag/n-type Si(100) diode. This a specular spectrum with the ion beam incident on the ultra thin film structure at an angle of  $45^\circ$ . Prior to obtaining this scattered spectrum the Ag top layer of the diode was sputter-cleaned using 500 eV  $Ar^+$  ions. There are two distinct features present in the spectrum shown in Fig. 6. The most pronounced and lowest energy peak is related to a QS collision. It agrees well with the binary collision approximation indicated by the dashed line. The broad high energy shoulder on this QS peak is consistent with a QD collision, indicated by the dashed-dotted line. However, based on our results obtained with the Ag(001) surface and the fact that multiple (111) orientations are expected for this surface, we can assume that multiple, out-of-plane zig-zag type trajectories also contribute to the scattered intensity. The measurements do confirm that our as-grown Ag layer is continuous and that the kinetic energy deposited in this system can be modeled using binary collision kinematics. Therefore we can use the scattering geometry to control the energy available for the excitation of hot electrons in this system. Further measurements will detect these excitations as currents induced within the diode.

## 4. Summary

In this study, we have probed the scattering of  $K^+$  and  $Cs^+$  ions from both a single crystal Ag(001) surface and from a Ag/n-type Si(100) Schottky diode. On the single crystal Ag surface, our  $K^+$  results are consistent with previous similar mass ratio results seen for Na–Cu scattering. In addition, classical trajectory simulations show that new low energy features observed in the scattered spectra arise due to the (110) orientation that was chosen for our incident beam. A binary collision treatment that accounts for the heavy atom nature of the  $Cs^+$  scattering is consistent with much of our data on the Ag(001) surface. However, an anomalous result for incident energies near 100 eV is observed. A more rigorous molecular dynamics treatment that can model the collective lattice dynamics that affect such slow moving projectiles is proposed. Finally,  $K^+$  scattering data were presented for a fabricated Schottky diode structure that incorporates an ultrathin Ag top layer. The scattered signal from this prototype device for hot electron detection exhibits energy loss that mimics that seen on the single crystal with an added complexity that most likely arises from its multiple (111) oriented domains.

## References

- [1] A.W. Kleyn, T.C.M. Horn, Phys. Rep. 199 (4) (1991) 192.
- [2] B.H. Cooper, E.R. Behringer, Low Energy Ion Surface Interactions, John Wiley and Sons, New York, 1994.
- [3] B.R. Cuenya, H. Nienhaus, E.W. McFarland, Phys. Rev. B 70 (11) (2004) 115322.
- [4] S. Glass, H. Nienhaus, Phys. Rev. Lett. 93 (16) (2004) 168302.
- [5] D. Krix, R. Nunthel, H. Nienhaus, Phys. Rev. B 75 (7) (2007) 073410.
- [6] H. Nienhaus, H.S. Bergh, B. Gergen, A. Majumdar, W.H. Weinberg, E.W. McFarland, Phys. Rev. Lett. 82 (2) (1999) 446.
- [7] S. Meyer, D. Diesing, A. Wucher, Phys. Rev. Lett. 93 (13) (2004) 137601.
- [8] D.A. Kovacs, T. Peters, C. Haake, M. Schlegelberger, A. Wucher, A. Golczewski, F. Aumayr, D. Diesing, Phys. Rev. B 77 (2008) 245432.
- [9] A. Schüller, S. Wethkam, H. Winter, Phys. Rev. Lett. 98 (1) (2007) 016103.
- [10] A. Schüller, H. Winter, Phys. Rev. Lett. 100 (9) (2008) 097602.
- [11] P. Rousseau, H. Khemliche, A.G. Borisov, P. Roncin, Phys. Rev. Lett. 98 (1) (2007) 016104.
- [12] G.F. Liu, Z. Sroubek, J.A. Yarmoff, Phys. Rev. Lett. 92 (21) (2004) 216801.
- [13] G.F. Liu, Z. Sroubek, P. Karmakar, J.A. Yarmoff, J. Chem. Phys. 125 (5) (2006) 054715.
- [14] T.C.M. Horn, A.D. Tenner, P.H. Chang, A.W. Kleyn, J. Electron Spectrosc. Relat. Phenom. 38 (1–4) (1986) 81.
- [15] T.C.M. Horn, P. Haochang, A.W. Kleyn, J. Vac. Sci. Technol. A 5 (4) (1987) 656.

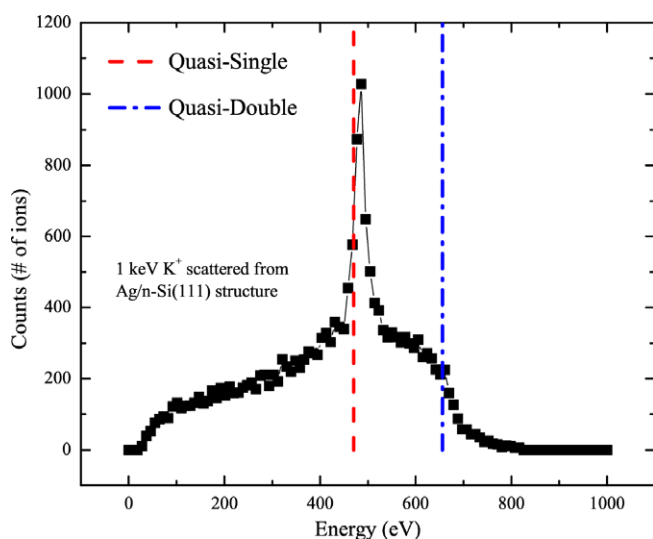


**Fig. 6.** A specular energy spectrum for 1 keV  $K^+$  ions scattered from a 20 nm Ag/n-type Si(100) device with an incident angle of  $45^\circ$ . The line connecting individual data points has been included as a guide. The QS and QD predictions are shown as calculated within the binary collision approximation.

- [16] T.C.M. Horn, H.C. Pan, P.J. Vandenhoek, A.W. Kleyn, Surf. Sci. 201 (3) (1988) 573.
- [17] T.C.M. Horn, U. Vanslooten, A.W. Kleyn, Chem. Phys. Lett. 156 (6) (1989) 623.
- [18] M.P. Ray, R.E. Lake, S.A. Moody, V. Magadala, C.E. Sosolik, Rev. Sci. Instr. 79 (7) (2008) 076106.
- [19] C.S. Jiang, H. Yu, C.K. Shih, P. Ebert, Surf. Sci. 518 (1&2) (2002) 63.
- [20] T. Tanikawa, I. Matsuda, T. Nagao, S. Hasegawa, Surf. Sci. 493 (1–3) (2001) 389.
- [21] M.H. Hoegen, T. Schmidt, G. Meyer, D. Winau, K.H. Rieder, Phys. Rev. B 52 (15) (1995) 10764.
- [22] C.A. DiRubio, R.L. McEachern, J.G. McLean, B.H. Cooper, Phys. Rev. B 54 (12) (1996) 8862.
- [23] D.M. Goodstein, S.A. Langer, B.H. Cooper, J. Vac. Sci. Technol. A 6 (3) (1988) 703.
- [24] M.P. Ray, R.E. Lake, C.E. Sosolik, Phys. Rev. B, submitted for publication.
- [25] C.E. Sosolik, B.H. Cooper, Nucl. Instr. and Meth. B 182 (1–4) (2001) 167.
- [26] M.C. Yang, C. Kim, H.W. Lee, H. Kang, Surf. Sci. 357&358 (1996) 595.
- [27] D.M. Goodstein, R.L. McEachern, B.H. Cooper, Phys. Rev. B 39 (18) (1989) 13129.
- [28] B. Gergen, H. Nienhaus, W.H. Weinberg, E.W. McFarland, Science 294 (5551) (2001) 2521.
- [29] S. Meyer, D. Diesing, A. Wucher, Phys. Rev. Lett. 93 (13) (2004) 137601.
- [30] A. Duvenbeck, O. Weingart, V. Buss, A. Wucher, Nucl. Instr. and Meth. B 255 (1) (2007) 281.
- [31] S. Meyer, C. Heuser, D. Diesing, A. Wucher, Phys. Rev. B 78 (3) (2008) 035428.
- [32] R.E. Lake, J.R. Puls, M.P. Ray, D.E. Dickel, A.M. Rao, C.E. Sosolik, Thin Solid Films, submitted for publication.